Dielectric approach to a dense charged boson gas at $T = 0$

J. C. Lee

Department of Chemistry and Physics, Northwestern State University, Natchitoches, Louisiana 71457
(Received 21 October 1974)

The generalized dielectric constant is calculated to the order next to the Bogoliubov approximation. This is done by using the analogy between the condensed boson system and a fictitious fermion system with spin degeneracy equal to the total number of particles (instead of two). From the zero of the dielectric constant, we have calculated the first-order correction to the Bogoliubov plasmon energy and the half linewidth of the plasmon states. The real part of the solution is examined from a graphical view point to show that up to the specified order of approximation there exists only one mode of elementary excitation. The screening of the system to a static impurity charge is shown to be exponential at a long distance. The response of the system to a static transverse vector potential shows a perfect Meissner effect at long- and short-wavelength limits. We have also examined the diagrammatic structure for the number of particles in condensate. We show that the series contains only terms of integer powers of $r_s^{3/4}$. The entire treatment is fully number conserving.

I. INTRODUCTION

Once the generalized dielectric constant is known, a complete description of the properties of a many-body system is possible.[1] For example, from the frequency- and wave-vector-dependent dielectric constant, one can calculate ground-state energy, excitation spectrum, dynamic and static structure functions, and others. Thus a perturbation calculation for the dielectric constant provides a very convenient microscopic theory of a many-body system.

A dielectric approach to a boson system was made, at the order of Bogoliubov approximation, by Hugenholtz and Pines.[2] Ma and Woo[3] calculated the dielectric constant to the next order of approximation and then, from the zero of the dielectric constant, calculated the first-order correction to the Bogoliubov excitation energy for a dense charged boson gas. The Ma-Woo formalism of Bose dielectric theory is significantly different in its structure from those of electron gas. Noticeably, it is required that several functions be introduced that are not found in the electron gas. This was necessary because of the c-number replacement of the condensate operators and the subsequent necessity to deal with incomplete vertices.

In a previous paper,[4] we have shown that the idea of fermion analogy due to Brandow[5] may be applied in a time-dependent manner to provide an extremely simple dielectric approach. This was done only at the zeroth order of approximation. It is the purpose of this paper to extend the theory to the first order.

As Brandow emphasized, the fermion analogy makes it possible to study a boson system along a line completely parallel to the corresponding normal fermion system. For example, we have shown previously[6] that the ring diagrams of a charged boson gas may be summed by using the same method that Gell-Mann and Brueckner[7] used for an electron gas. In a continuing effort, we apply in this paper the techniques of DuBois[8] to calculate the dielectric constant of a charged boson gas.

The only task is to calculate the irreducible polarization part $\pi(\vec{p}, p_0)$. This can be done without introducing at the outset the chemical potential, the depletion factor, and those functions that are unique in the boson formalism of Ma and Woo but absent in the electron gas. While Ma and Woo introduce various building blocks and then "build" the irreducible polarization part, the equivalent work is done in our formalism "automatically" by drawing diagrams in the same way as DuBois does and then carrying out the integrations that the diagram rules require. The diagram rules are the same as those of a normal fermion system[9] except that the spin degeneracy of each momentum state is equal to the total number of particles and consequently the Fermi momentum is zero. To those who find it annoying to handle the tangle of μ and N_0, in particular the tangle of μ on μ itself and the similar tangle of N_0, our procedure should prove simple and straightforward.

In the zeroth order of approximation, $\pi(\vec{p}, p_0)$ is approximated by the simple bubble diagram (see Fig. 1). The result[4] is reviewed in Sec. II. In the first order of approximation, the electron and the hole (the virtual pair) are allowed to interact with each other or with the Fermi sea (condensate). Thus we first attach an effective potential line (a direct interaction plus the virtual polarization effect of the medium) between the two directed lines or just to one of them in the zeroth-order diagram resembling a bump [see Figs. 2(a)–2(c)]. For an electron gas, this would be sufficient for the first order of approximation. For bosons, however,
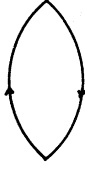
FIG. 1. Zeroth-order irreducible polarization part $\pi^{(0)}(p)$; for this diagram, $l = 0$.

one has to include some additional diagrams. This is a consequence of the peculiar Fermi sea made out of the single state $\vec{p} = 0$ unlike the real Fermi sea of electron gas. The additional diagrams are shown in Figs. 2(d) and 2(e). The reason why they must be included in the first order of approximation is explained in Sec. II. The contribution of these first-order diagrams is then calculated in Sec. III. The resultant dielectric constant is set to zero in Sec. IV; the real part gives the correction to the zeroth-order plasmon energy, and the imaginary part the linewidth of the excited states. The real part of the equation is discussed from a graphical viewpoint. Up to the first order of approximation, we prove that there is only one solution for the elementary excitation. The second branch of Carmi and Lock[10] is absent.

Section IV is devoted to study the response of the system to weak external fields. The induced charge distribution around a static impurity charge is shown to be screened at a long distance exponentially.[11] A calculation on the transverse current induced by a weak transverse vector potential shows a perfect Meissner effect in the two limits of long and short wavelength, a result first obtained by Fetter.[12] We have also derived the irreducible part of the longitudinal current correlation function. The result is identical with that of Ma and Woo.

Throughout this paper, we will remain in a fixed-N formalism. All expectation values will be taken in the ground state with a fixed particle number. The operators for which expectation values will be taken contain equal numbers of creation and annihilation operators. At no stage will the condensate operators be replaced by the c number $N_0^{1/2}$. This is done by introducing a "hole" part in the free-particle Green's function [see (3)]. The Hamiltonian is invariant to the gauge transformation $(a \rightarrow ae^{ix})$ and so are all the results of the expectation values taken in this paper. The gauge symmetry does not have to be broken for reasons mentioned above and thus we are able to treat a condensed boson system without introducing the so-called "source field."

The condensate density of a boson system is an important variable. Although there is no doubt

that the condensation is near complete in the high-density limit, there has been some difference among authors in the r_s expansion. The work of Schick and Wu[13] is unique in this regard because they claim a term of order $r_s^{9/8}$, which is absent, for example, in the work of Woo and Ma.[14] We comment on this subject matter in Appendix A, where we show that the condensate density may be computed to any order of approximation. The procedure is unique in that there is no tangle with N_0 itself or with μ. This is not the case when the condensate operators are replaced by c number $N_0^{1/2}$. Appendix B is devoted to show a similar perturbation calculation for the chemical potential. In Appendix C, we discuss the relationship to the formalism of Hugenholtz and Pines.

II. ZEROTH-ORDER APPROXIMATION AND DIAGRAM CLASSIFICATION

A. Zeroth-order approximation

The main function of interest is the density-density correlation function defined by

$$F(p) = -i \int dt\, e^{ip_0 t} \langle T(\rho_{\vec{p}}(t)\rho_{\vec{p}}^+(0)) \rangle , \qquad (1)$$

where $p = (\vec{p}, p_0)$; the angular brackets represent the ground-state expectation value; $\rho_{\vec{p}} = \sum_{\vec{q}} a_{\vec{p}+\vec{q}}^\dagger a_{\vec{q}}$ and the a's are annihilation operators. The spin variable is not shown explicitly, but let us keep in mind that for each momentum state there are N spin degeneracies. The Fermi sea is composed of the single-state $\vec{p} = 0$ with N spin degeneracies, and therefore summation over the states in the Fermi sea is performed by multiplying by N. This provides a remarkable simplicity in calculating diagram contributions in boson problems.

The function F, which is a geometric series of the irreducible polarization part $\pi(p)$, is given by

$$F(p) = \frac{\pi(p)}{1 - \nu_{\vec{p}}\pi(p)} , \qquad (2)$$

where $\nu_{\vec{p}}$ is the Fourier transform of the interparticle potential. We have set $\hbar = 1$. In the high-density limit, it is sufficient to evaluate the leading term of π shown in Fig. 1. The directed lines in this and other diagrams in our method represent

$$G_0(p) = \frac{\eta_{\vec{p}}}{p_0 - T_{\vec{p}} + i\delta} + \frac{1 - \eta_{\vec{p}}}{p_0 - i\delta}$$

$$\equiv G_0^+(p) + G_0^-(p) , \qquad (3)$$

where $T_{\vec{p}} = p^2/2m$; and $\eta_{\vec{p}} = 1$ if $\vec{p} \neq 0$, and 0 if $\vec{p} = 0$. The contribution of Fig. 1 is

$$\pi^{(0)}(p) = i(-N) \int \frac{d^4q}{(2\pi)^4}\, (p+q)G_0(q)$$

$$= n[G_0^+(p) + G_0^+(-p)] \qquad (4)$$

$$= 2nT_{\vec{p}}/(p_0 - T_{\vec{p}} + i\delta)(p_0 + T_{\vec{p}} - i\delta) ,$$

where $n = N/\Omega$ is the particular number density; $-N$ is due to the Fermi loop. As in (4) we will replace the integral $\int d^3q/(2\pi)^3$ by $(1/\Omega)\sum_{\vec{q}}$ whenever $1 - \eta_{\vec{q}}$ is encountered. Substituting (4) into (2), we have

$$F^{(0)}(p) = 2nT_{\vec{p}}/(p_0 - E_{\vec{p}} + i\delta)(p_0 + E_{\vec{p}} - i\delta) , \qquad (5)$$

where $E_{\vec{p}}$, given by

$$E_{\vec{p}} = (T_{\vec{p}}^2 + 2nv_{\vec{p}}T_{\vec{p}})^{1/2} , \qquad (6)$$

is the excitation energy of zeroth order. There are many different derivations of this well-known Bogoliubov energy, but perhaps ours is the simplest one. This simplicity may also be found in the next order of approximation.

Closely related to F is the effective potential,

$$v_{\text{eff}}(p) = v_{\vec{p}}^2 F^{(0)}(p) + v_{\vec{p}}$$

$$= 2nv_{\vec{p}}^2 T_{\vec{p}}/(p_0 - E_{\vec{p}} + i\delta)(p_0 + E_{\vec{p}} - i\delta) + v_{\vec{p}}$$

$$\equiv v'_{\text{eff}} + v_{\vec{p}} . \qquad (7)$$

The superscript zero has been omitted in (6) and (7) because they appear very frequently later on and we wish to simplify the notation.

B. Diagram classification

Before we proceed to calculate $\pi^{(1)}$, let us explain the diagram classification. As was mentioned earlier, for every Fermi loop, a factor $-N$ is multiplied. Therefore in the limit $N \to \infty$, the number of Fermi loops s will dictate which diagrams are to be chosen. For a given number of interaction lines n, s will determine the importance of the diagram. In the zeroth order of approximation, $s = 1$ and $n = 0$. Let us write it as $s = n + 1$. In the succeeding orders, $s = n$, $s = n - 1$, $s = n - 2$, and so on. Inspecting a few diagrams and remembering that our hole lines carry momentum zero, it is clear that $n - s$ is equal to the number of independent momenta l. This is again a consequence of the peculiar Fermi sea. Thus the order of approximation is determined by l alone. For Fig. 1, $l = 0$. The diagrams with $l = 1$ are shown in Fig. 2; and those with $l = 2$ are shown in Fig. 3. In Fig. 3 only structures of diagrams are shown. The diagrams are all familiar from DuBois but are classified in a slightly different way for bosons.

What is presented above is, however, only a formal classification and it is not obvious at this point under what condition diagrams of a given order are more important than those of higher orders. We show in Sec. IV that for a charged boson gas $v_{\vec{q}}\pi^{(1)}(q)$ is of order $(r_s^{3/4})^l$. Thus for a dense charged boson gas the above classification is meaningful and r_s serves as the expansion parameter.

III. FIRST-ORDER APPROXIMATION: FIRST ORDER IRREDUCIBLE POLARIZATION

In the first order of approximation, the irreducible polarization parts with one independent momentum variable are added to $\pi^{(0)}$. The diagrams to be calculated are shown in Fig. 2. Unlike in the electron gas, it is quite easy to calculate the *exact* contributions of these diagrams. First consider (a). It is given by

$$\pi_a^{(1)}(p) = i^2(-N) \int \frac{d^4q_1}{(2\pi)^4} \int \frac{d^4q_2}{(2\pi)^4} G_0(q_1)G_0(p + q_1)$$

$$\times G_0(q_2)G_0(p + q_2)v_{\text{eff}}(q_2 - q_1) , \qquad (8)$$

where $-N$ is again due to the Fermi loop. The integral is nonvanishing only when one of the G_0's is G_0^- and the rest are G_0^+. Performing the integration for the frequency variable in the G_0^-,

$$\pi_a^{(1)}(p) = 2iG_0^+(p) \int \frac{d^4q}{(2\pi)^4} G_0^+(p + q)G_0^+(q)nv_{\text{eff}}(q)$$

$$+ (p \to -p) , \qquad (9)$$

where $p \to -p$ indicates that the term may be obtained from the preceding term by replacing $p = (\vec{p}, p_0)$ by $-p$. It proves wise to defer the remaining q_0 integration until the rest of $\pi^{(1)}$'s are examined. In a similar way,

$$\pi_b^{(1)}(p) = i \int \frac{d^4q}{(2\pi)^4} [G_0^+(q)]^2 G_0^+(p + q)nv'_{\text{eff}}(q)$$

$$+ i[G_0^+(-p)]^2 \int \frac{d^4q}{(2\pi)^4} G_0^+(-p + q)nv'_{\text{eff}}(q)$$

$$+ n[G_0^+(p)]^2(-\mu^{(1)}) + G_0^+(p)n_0^{(1)} , \qquad (10)$$
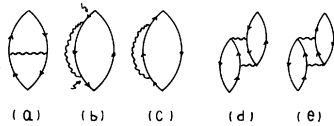

FIG. 2. First-order irreducible polarization part $\pi^{(1)}(p)$. For these diagrams, $l = 1$. The wiggly lines represent $v_{\text{eff}}(p)$ given by (7). The curly arrows have been drawn here for a purpose of reference in Appendix C.
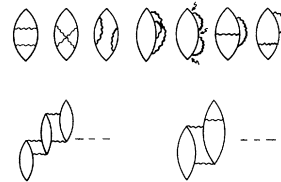

FIG. 3. Second-order irreducible polarization part $\pi^{(2)}(p)$. For these diagrams, $l = 2$. The wiggly lines represent $v_{\text{eff}}(p)$ given by (7). The diagrams not explicitly shown in the second line may be obtained by connecting three (two) bubbles using four (three) wiggly lines in all possible ways such that the diagrams remain irreducible.

where

$$\mu^{(1)} = i \int \frac{d^4q}{(2\pi)^4} G_0^+(q) \nu'_{\text{eff}}(q) \tag{11}$$

and

$$n_0^{(1)} = -in \int \frac{d^4q}{(2\pi)^4} [G_0^-(q)]^2 \nu'_{\text{eff}}(q) . \tag{12}$$

In Appendixes A and B, we identify $\mu^{(1)}$ and $n_0^{(1)}$ as the first-order terms of chemical potential and the condensate density, respectively. The last two terms of (10) arise when the two G_0's indicated by arrows in Fig. 2(b) are G_0^- and the rest are G_0^+.

The corresponding integral

$$i^2 \left(\frac{-N}{\Omega} \right) \int \frac{dq_0}{(2\pi)} \int \frac{d^4k}{(2\pi)^4} G_0^+(\vec{p}, p_0 + q_0) [G_0^-(q_0)]^2$$

$$\times G_0^+(\vec{k}, k_0 + q_0) \nu'_{\text{eff}}(k) \tag{13}$$

yields the two terms. This is a time-dependent version of the first-order hole-line renormalization thoroughly explained in Ref. 5. This point is further explained in Appendix C.

The contributions of the rest of the diagrams are also calculated by a straightforward algebra with the result:

$$\pi_c^{(1)}(p) = \pi_b^{(1)}(-p) , \tag{14}$$

$$\pi_d^{(1)}(p) = 2iG_0^+(p)n^2 \int \frac{d^4q}{(2\pi)^4} G_0^+(p-q)G_0^+(q-p)G_0^+(q)\nu_{\text{eff}}(q-p)\nu_{\text{eff}}(q) + (p \rightarrow -p)$$

$$+ in^2 \int \frac{d^4q}{(2\pi)^4} [G_0^+(p+q)]^2 [G_0^+(q)]^2 \nu_{\text{eff}}(p+q)\nu_{\text{eff}}(q)$$

$$+ 2iG_0^+(p)G_0^+(-p)n^2 \int \frac{d^4q}{(2\pi)^4} G_0^+(q)G_0^+(p+q)\nu_{\text{eff}}(q)\nu_{\text{eff}}(p+q)$$

$$+ i[G_0^+(p)]^2 n^2 \int \frac{d^4q}{(2\pi)^4} [G_0^+(p+q)]^2 \nu_{\text{eff}}(q)\nu_{\text{eff}}(p+q) + (p \rightarrow -p) , \tag{15}$$

$$\pi_e^{(1)}(p) = 2iG_0^+(p)n^2 \int \frac{d^4q}{(2\pi)^4} [G_0^+(p+q)]^2 G_0^+(q)\nu_{\text{eff}}(q)\nu_{\text{eff}}(p+q) + (p \rightarrow -p)$$

$$+ in^2 \int \frac{d^4q}{(2\pi)^4} G_0^+(q)G_0^+(-q)G_0^+(p+q)G_0^+(-p-q)\nu_{\text{eff}}(q)\nu_{\text{eff}}(p+q)$$

$$+ 2iG_0^+(p)G_0^+(-p)n^2 \int \frac{d^4q}{(2\pi)^4} G_0^+(q)G_0^+(-q)\nu_{\text{eff}}(q)\nu_{\text{eff}}(p+q)$$

$$+ i[G_0^+(p)]^2 n^2 \int \frac{d^4q}{(2\pi)^4} G_0^+(-q)G_0^+(p+q)\nu_{\text{eff}}(-q)\nu_{\text{eff}}(p+q) + (p \rightarrow -p) . \tag{16}$$

Several combinations of G_0^+'s and ν_{eff} appear frequently. They are

$$G_{11}'(q) \equiv [G_0^+(q)]^2 n\nu_{\text{eff}}(q) ,$$
$$G_{12}(q) \equiv G_0^+(q)G_0^+(-q)n\nu_{\text{eff}}(q) = -n\nu_q / (q_0 - E_{\vec{q}} + i\delta)(q_0 + E_{\vec{q}} - i\delta) . \tag{17}$$

It is easy to show that

$$G_{11}(q) \equiv G_{11}'(q) + G_0^+(q) = \frac{f_{\vec{q}} + 1}{q_0 - E_{\vec{q}} + i\delta} - \frac{f_{\vec{q}}}{q_0 + E_{\vec{q}} - i\delta} ,$$

$$G_0^+(q)\nu'_{\text{eff}}(q) = \nu_{\vec{q}} [G_{11}'(q) + G_{12}(q)] , \tag{18}$$

$$G_0^+(q)\nu_{\text{eff}}(q) = \nu_{\vec{q}} [G_{11}(q) + G_{12}(q)] = \frac{\nu_{\vec{q}}}{2E_{\vec{q}}} \left[\frac{T_{\vec{q}} + E_{\vec{q}}}{q_0 - E_{\vec{q}} + i\delta} - \frac{T_{\vec{q}} - E_{\vec{q}}}{q_0 - E_{\vec{q}} + i\delta} \right] ,$$

where

$$f_{\vec{q}} = (T_{\vec{q}} - E_{\vec{q}} + n\nu_{\vec{q}})/2E_{\vec{q}} . \tag{19}$$

Using the above identities, one can combine $\pi_a^{(1)} + \pi_e^{(1)}$ and $\pi_b^{(1)} + \pi_c^{(1)} + \pi_d^{(1)}$, and then carry out the final q_0 integration. We find, after a simple algebra,

$$\pi^{(1)}(p) = G_0^+(p)P(p) + (p \rightarrow -p) + G_0^+(p)G_0^+(-p)U(p) + (p \rightarrow -p) + \theta(p) + (p \rightarrow -p) + [G_0^+(p)]^2 \phi(p) + (p \rightarrow -p), \tag{20}$$

with

$$P(p) = n_0^{(1)} + \frac{1}{2} \int \frac{d^3q}{(2\pi)^3} \, n\nu_{\vec{q}}[(\lambda_q - 1/\lambda_{q+p} - \lambda_q \lambda_{q+p} + 1)K^+ + (\lambda_q - 1/\lambda_{q+p} + \lambda_q \lambda_{q+p} - 1)K^-] \,,$$

$$U(p) = \frac{1}{4} \int \frac{d^3q}{(2\pi)^3} \, n\nu_{\vec{q}}(\lambda_{q+p} - 1/\lambda_{q+p}) + \frac{1}{2} \int \frac{d^3q}{(2\pi)^3} \, n\nu_{\vec{q}}[n\nu_{q+p}(1 - \lambda_q \lambda_{q+p}) + n\nu_q(\lambda_q/\lambda_{q+p} - \lambda_q \lambda_{q+p})]K^+ \,,$$

$$\theta(p) = -\frac{1}{8} \int \frac{d^3q}{(2\pi)^3} \, (1/\lambda_q \lambda_{q+p} + \lambda_q \lambda_{q+p} - 2)K^+ \,,$$

$$\phi(p) = \frac{1}{4} \int \frac{d^3q}{(2\pi)^3} \, n\nu_q (1/\lambda_{q+p} + \lambda_{q+p} - 2) - n\mu^{(1)}$$

$$+ \frac{1}{4} \int \frac{d^3q}{(2\pi)^3} \, n\nu_{\vec{q}}\{[n\nu_{\vec{q}}(2\lambda_q - \lambda_q \lambda_{q+p} - \lambda_q/\lambda_{q+p}) + n\nu_{q+p}(2\lambda_q - \lambda_{q+p} - 1)]K^+$$

$$+ [n\nu_{\vec{q}}(2\lambda_q + \lambda_q \lambda_{q+p} + \lambda_q/\lambda_{q+p}) + n\nu_{q+p}(2\lambda_q + \lambda_q \lambda_{q+p} + 1)]K^-\} \,, \tag{21}$$

where

$$(K^+, K^-) = \left(\frac{1}{p_0 + E_q + E_{q+p} - i\delta}, \; \frac{1}{p_0 - E_q - E_{q+p} + i\delta} \right) \,; \qquad \lambda_q = T_q / E_q$$

is the zeroth-order structure factor. In terms of λ_q, (11) and (12) may be written as

$$\mu^{(1)} = \frac{1}{2} \int n^{-1} \frac{d^3q}{(2\pi)^3} \, (\lambda_q - 1) n\nu_{\vec{q}} \,, \tag{22}$$

$$n_0^{(1)} = -\frac{1}{4} \int \frac{d^3q}{(2\pi)^3} \frac{(\lambda_q - 1)^2}{\lambda_q} \,. \tag{23}$$

Now we have obtained the dielectric constant to the first order of approximation,

$$\epsilon(p) = 1 - \nu_{\vec{p}}[\pi^{(0)}(p) + \pi^{(1)}(p)] \,. \tag{24}$$

In spite of the remarkable difference between bosons and fermions, we have derived a boson result following more simple and straightforward procedure known for fermions.

IV. ELEMENTARY EXCITATION

A. Plasmon excitation energy

The excitation energy may be determined from the zero of the dielectric constant. Thus we set

$$\alpha_{\vec{p}}(p_0) \equiv \nu_{\vec{p}}\pi(\vec{p}, p_0) = 1 \,. \tag{25}$$

In the zeroth order of approximation, (25) is solved trivially with the result given by (6). Still it is instructive to plot $\alpha_{\vec{p}}^{(0)}$ against p_0. The graph is sketched in Fig. 4(a). The solution is determined by the intersection with ordinate value of unity. There is only one intersection and thus there is only one mode of elementary excitation at the zeroth order. We will show that this is also true in the next order of approximation. The elementary excitation is called plasmon. Unlike in the electron gas, there is no continuum of intersections at the zeroth order. The boson analog of the electron-hole pair excitation does not exist.

In the first order of approximation, we have

$$\alpha_{\vec{p}}(p_0) = \alpha_{\vec{p}}^{(0)}(p_0) + \Delta\alpha_{\vec{p}}^{(1)}(p_0) \,, \tag{26}$$

where

$$\Delta\alpha_{\vec{p}}^{(1)}(p_0) = \nu_{\vec{p}}\pi^{(1)}(\vec{p}, p_0) \,.$$

How does the additional term $\Delta\alpha^{(1)}$ affect the graphical solution? The curve of $\Delta\alpha_{\vec{p}}^{(1)}$ plotted against p_0 must be examined. In particular, we wish to examine whether or not there is any possibility of more than one intersection in the range $p_0 < 2\omega_{pl}$ where $\omega_{pl} = (4\pi n e^2/m)^{1/2}$. According to Carmi and Lock,[10] there is a second mode of *elementary* excitation, which is different from the plasmon; it approaches zero as $\vec{p} \to 0$ unlike the plasmon. For this reason, we computed $\Delta\alpha^{(1)}$ as a function of p_0 using a computer. We did this for several values of $\vec{p}$ with the result sketched in Fig. 4(b). Note that there is a pole at $p_0 = T_p$ as may be seen from (20). The value of $\Delta\alpha_{\vec{p}}^{(1)}$ is minus infinity near the pole and then increases monotonically as p_0 decreases from $p_0 = T_p$. It also increases monotonically as p_0 increases from $p_0 = T_p$, but it is soon interrupted by the region of two-plasmon continuum. By adding $\Delta\alpha^{(1)}$ to $\alpha^{(0)}$, it is quite clear that there is no possibility of more than one intersection in the range $p_0 < 2\omega_{pl}$. Had $\Delta\alpha^{(1)}$ turned out to be pos-
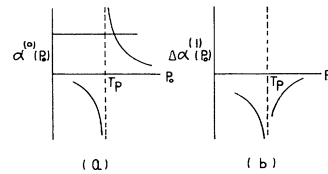

FIG. 4. Sketches for (a) $\alpha_{\vec{p}}^{(0)}(p_0)$, (b) $\Delta\alpha_{\vec{p}}^{(1)}(p_0)$. We computed $\Delta\alpha_{\vec{p}}^{(1)}(p_0)$ with $|\vec{p}|$ fixed at several values using a computer. In all cases, the result showed the characteristics sketched (not plotted) in (b).
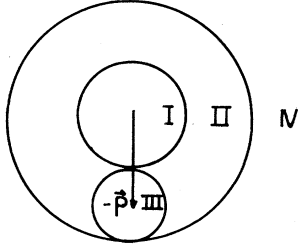
FIG. 5. Integral domain was divided in this way to avoid the apparent (not real) singularity that occurs at $\vec{q} = -\vec{p}$ in evaluating ΔE_p and $\Delta \alpha_{\vec{p}}^{(1)}(p_0)$.

itive for $p_0 < T_p$, it might have been possible to have a second intersection. Thus we conclude that there is no second branch of elementary excitation in a dense charged boson gas.

The effect of $\Delta \alpha^{(1)}$ to the dispersion curve is clear: It pushes the point of intersection to a smaller value of p_0. Now let us find this shift. By writing $\pi^{(1)} = \pi_R^{(1)} + i\pi_I^{(1)}$, the condition (25) yields,

$$p_0^2 - E_p^2 - (p_0^2 - T_p^2)\nu_p\pi_R^{(1)} - i(p_0^2 - T_p^2)\nu_p\pi_I^{(1)} = 0 . \quad (27)$$

The correction ΔE_p is obtained from the real part of the solution,

$$p_0 = (E_p + \Delta E_p) + i\gamma_{\vec{p}} . \quad (28)$$

Now we show that $\nu_{\vec{p}}\pi^{(1)}$ is of order $r_s^{3/4}$. To see this, make the familiar change of variable,

$$|\vec{q}| = (4\pi n/a_0)^{1/4}|\vec{t}| ,$$
$$n = (3/4\pi)(r_s a_0)^{-3} , \quad (29)$$

where a_0 is the Bohr radius. (Note that we have here n, not n_0.) Then we find

$$T_{\vec{q}} = (\tfrac{1}{2}t^2) \text{ Ry}' ,$$
$$E_{\vec{q}} = (\tfrac{1}{4}t^4 + 1)^{1/2} \text{ Ry}' ,$$
$$n\nu_{\vec{q}} = t^{-2} \text{ Ry}' , \quad (30)$$
$$n^{-1}d^3q = g\,d^3t ,$$

where $\text{Ry}' = 2 \times 3^{1/2}r_s^{-3/2} \text{ Ry}$ and $g = 4\pi 3^{-1/4} r_s^{3/4}$. Recall that $\pi^{(1)}$ is written in terms of the three functions T_q, E_q, and $n\nu_q$. According to (30) the r_s dependences of these functions are identical. Since $\pi^{(1)}$ contains one independent variable, $\nu_q\pi^{(1)} = n\nu_q n^{-1}\pi^{(1)}$ is of order $r_s^{3/4}$. In general, $\nu_q\pi^{(l)}$ has l-independent momentum variables and therefore is of order $(r_s^{3/4})^l$.

Since there is only one solution for $p_0 < 2\omega_{pl}$ and $\nu_p\pi^{(1)}$ is of order $r_s^{3/4}$, it is safe in the high-density limit to iterate the real part of (27). The result is

$$\Delta E_p = (T_p n^2 \nu_p^2/E_p)n^{-1}\pi_R^{(1)}(\vec{p}, E_p) . \quad (31)$$

We have evaluated (31) using a computer. Note that $\pi_R^{(1)}$ contains terms of form $\int d^3q\, f(\vec{q}, \vec{p})|\vec{q} + \vec{p}|^{-2}$. Thus, the integrand becomes singular at $\vec{q} = -\vec{p}$. We have avoided this apparent (not real) singularity by dividing the region of integration into four as shown in Fig. 5 and then in III, where the singular point is located, by making a change of variable $\vec{q} + \vec{p} = \vec{q}'$. The result is shown in Fig. 6 and is in agreement with Ma and Woo.

B. Damping of plasmon state

The elementary excitation E_p at the zeroth order represents a well-defined excited state. At the first order, however, the solution to (27) has an important imaginary part and thus the linewidth is no longer zero for all momenta. The imaginary part (half-linewidth) is given by

$$\gamma_{\vec{p}}^{(1)} = (T_p n^2 \nu_p^2/E_p) n^{-1}\pi_I^{(1)}(\vec{p}, E_p)$$

$$= -\pi \int n^{-1}\frac{d^3q}{(2\pi)^3} \delta(E_{\vec{p}} - E_{-\vec{q}} - E_{\vec{q}+\vec{p}})\{(\tfrac{1}{2}\lambda_p n\nu_p n\nu_q)(\lambda_q\lambda_{q+p} - 1) + (\tfrac{1}{2}n\nu_p n\nu_q)(\lambda_q - 1/\lambda_{q+p})$$

$$+ \tfrac{1}{8}\lambda_p(n\nu_p)^2(1/\lambda_q\lambda_{q+p} + \lambda_q\lambda_{q+p} - 2) - (n\nu_p n\nu_q/4E_p)[n\nu_{q+p}(\lambda_q\lambda_{q+p} - 1) + n\nu_q(\lambda_q\lambda_{q+p} - \lambda_q/\lambda_{q+p})]$$

$$+ \tfrac{1}{8}(\lambda_p + 1/\lambda_p)n\nu_q[n\nu_{q+p}(\lambda_q\lambda_{q+p} + 1) + n\nu_q(\lambda_q\lambda_{q+p} + \lambda_q/\lambda_{q+p})] + \tfrac{1}{2}n\nu_q\lambda_q(n\nu_q + n\nu_{q+p})\} . \quad (32)$$

We have evaluated this integral using a computer. The result is presented in Fig. 7. The width is zero up to the critical momentum ($t = 2$) and then increases very rapidly to a maximum and then decreases gradually to zero as momentum increases to infinity. The plasmons near $t = 2.2$ is especially unstable against the two-plasmon continuum. This is similar in character to the diffuse plateau in liquid ^{4}He appearing after the roton dip. For very large momenta, a plasmon is identical to a free particle and is a well-defined state.

For $p_0 > 2\omega_{pl}$ there is a continuum of intersec-

tions. These intersections represent the excited states containing two plasmons, one with momentum $-\vec{q}$ and the other with momentum $\vec{q} + \vec{p}$. Figure 8 depicts the two possible ways these intersections may actually occur. It is not hard to show that it is (a).

V. LINEAR RESPONSE

A. Response to a static impurity charge

We examine here the screening effect of the system to a static impurity of charge Ze. The induced

charge density is given by

$$\delta\langle n(p)\rangle = F^R(p)Ze\nu_{\vec{p}}^- 2\pi\delta(p_0) , \qquad (33)$$

where F^R is the linear density response function which may be obtained by taking the retarded version[9] from F.

It has been shown by Fetter[11] that the asymptotic screening is exponential ($\propto e^{-\lambda r}$) above the phase

$$\delta\langle n(r)\rangle = \frac{Ze}{2\pi^2 r}\int_0^\infty dp \sin(pr)p\nu_p \frac{\pi^{(0)}(\vec{p},0)+\pi^{(1)}(\vec{p},0)}{1-\nu_{\vec{p}}^-[\pi^{(0)}(\vec{p},0)+\pi^{(1)}(\vec{p},0)]} , \qquad (34)$$

where

$$\pi^{(0)}(\vec{p},0) = -2n/T_{\vec{p}}^- ,$$

$$\pi^{(1)}(\vec{p},0) = \frac{2}{T_{\vec{p}}^-}\left\{\int\frac{d^3q}{(2\pi)^3}n\nu_q(\lambda_q\lambda_{q+p}-1)(E_q+E_{q+p})^{-1}-n_0^{(1)}\right\}-\frac{1}{4}\int\frac{d^3q}{(2\pi)^3}\left(\frac{1}{\lambda_q\lambda_{q+p}}+\lambda_q\lambda_{q+p}-2\right)(E_q+E_{q+p})^{-1}$$

$$-\frac{2}{T_p^2}\left\{\int\frac{d^3q}{(2\pi)^3}n\nu_q(n\nu_q+n\nu_{q+p})\lambda_q\lambda_{q+p}(E_q+E_{q+p})^{-1}-\frac{1}{2}\int\frac{d^3q}{(2\pi)^3}n\nu_q(\lambda_{q+p}-1)+n\mu^{(1)}\right\} . \qquad (35)$$

Since the integrand in (34) is even in $p=|\vec{p}|$, it may be written as

$$\delta\langle n(r)\rangle = \frac{Ze}{2\pi^2 r}\frac{1}{2i}\int_{-\infty}^\infty dp\, e^{ipr}p\nu_p$$

$$\times\frac{\pi^{(0)}(\vec{p},0)+\pi^{(1)}(\vec{p},0)}{1-\nu_{\vec{p}}^-[\pi^{(0)}(\vec{p},0)+\pi^{(1)}(\vec{p},0)]} . \qquad (36)$$

The integrand is an analytic function of p on the real axis and therefore the integration may be performed by closing the contour in the upper half-plane. The zero of the denominator of the integrand in (36) is given by

$$T_p^3+\omega_{pl}^2 T_p-\tfrac{1}{2}\omega_{pl}^2 T_p^2 n^{-1}\pi^{(1)}(\vec{p},0) = 0 , \qquad (37)$$

where $\omega_{pl}^2 = 2nT_{\vec{p}}^-\nu_{\vec{p}}^-$. (37) has solutions in the upper half-plane. Recall that we have shown numerically that $\pi^{(1)}(\vec{p},0)$ is negative in Sec. IV. Thus there are simple poles in the upper half-plane and the exponential nature of the screening is established. It is certainly possible to evaluate (34) numerically, but we did not feel such numerical result would be interesting enough to justify the cost.

In the extreme high-density limit, $\pi^{(1)}$ in (37) may be ignored; the simple poles occur then at $p = \sqrt{2}\lambda e^{i\pi/4}$ and $p = \sqrt{2}\lambda e^{i3\pi/4}$, where $\lambda = (4\pi n/a_0)^{1/4}$. The contour integral of (36) is performed easily with the result

$$\delta\langle n)r)\rangle = -(Ze/2\pi r)\lambda^2 e^{-\lambda r}\sin(\lambda r) . \qquad (38)$$

The total induced charge is $-Ze$ as may be seen by integrating (38). When $\pi^{(1)}$ is included, this perfect screening effect still persists in the long wavelength limit. This follows from

transition temperature but becomes algebraic ($\propto 1/r^5$) at the transition temperature. The screening below the transition temperature in the condensed phase is an interesting open question. Although we do not have a complete answer, the character of screening at $T=0$ is easy to find.

By taking the inverse Fourier transform, we have

$$\lim_{p\to 0}\frac{1}{\epsilon(\vec{p},0)} = 0 , \qquad (39)$$

where (35) is used.

B. Response to a static transverse vector potential

It has been shown by Fetter[12] that a dense charged boson gas exhibits a perfect Meissner effect at the limits $\vec{p}\to 0$ and $\vec{p}\to\infty$. We have nothing new to add. However, since this interesting subject matter may be seen only after a few steps, we wish to present here what might be called a diagrammatic version of Fetter's derivation.

The paramagnetic term of the induced current may be found from the retarded version of the current correlation function defined by

$$\mathcal{P}_{ij}(p) = -i\int dt\, e^{ip_0 t}\langle T(J_{-\vec{p}}^i(t)J_{\vec{p}}^j(0))\rangle , \qquad (40)$$
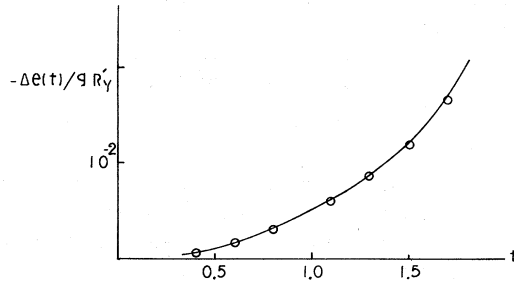

FIG. 6. Numerical result of ΔE_p. The solid line represents the result of Ma and Woo and the circle the result of (20). Our result is slightly lower than that of Ma and Woo but the difference is well within the numerical error.
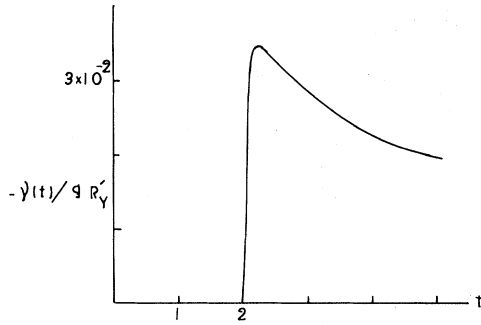
FIG. 7. Half-linewidth of the plasmon states. Note that (31) contains a Dirac function. As a consequence of evaluating such an integral numerically, the actual numerical results were somewhat scattered around this curve.

where (i, j) represent the spatial components of the *unperturbed* current operator

$$\vec{J}_{\vec{p}} = \frac{e}{m}\sum_{\vec{q}} (\vec{q} + \tfrac{1}{2}\vec{p})a_{\vec{q}}^{\dagger} a_{\vec{p}+\vec{q}} \ . \tag{41}$$

The total induced current is then given by

$$j_{\vec{p}}^{k}(p) = -\frac{c}{4\pi}\sum_{l=1}^{3} K_{kl}(p)A_l(p) \ , \tag{42}$$

where

$$K_{kl}(p) = (4\pi n e^2/mc^2)\delta_{k,l} + (4\pi/c^2)\varphi_{kl}^R(p) \ . \tag{43}$$

The function $\varphi_{ij}(p)$ may be obtained in the same way as for F, but the fact that the two external vertices are $\vec{J}$ instead of ρ requires an extra amount of bookkeeping work. The London gauge and the cylindrical symmetry around $\vec{p}$, however, substantially simplify the problem by eliminating many diagrams. In particular, all of the reducible diagrams make no contribution; only irreducible diagrams Π_{ij} contribute. Π_{ij} may be calculated from Figs. 1 and 2. Among many terms, only the term that correspond to the $\theta(p)$ term in $\pi^{(1)}$ survives and the rest make no contribution. To see this in more detail, the zeroth-order diagram is given by

$$\Pi_{ij}^{(0)} = \frac{e^2}{4m^2}\ \frac{2nT_p}{(p_0 - T_p + i\delta)(p_0 + T_p - i\delta)}\ p_i p_j \ . \tag{44}$$

Clearly it makes no contribution. Each term of $\Pi_{ij}^{(1)}$ is in either one of the following three forms:

$$\int \frac{d^3q}{(2\pi)^3} f(\vec{q}, \vec{p})q_i p_j \ ,$$

$$\int \frac{d^3q}{(2\pi)^3} f(\vec{q}, \vec{p})p_i q_j \ ,$$

$$\int \frac{d^3q}{(2\pi)^3} f(\vec{q}, \vec{p})q_i q_j \ .$$

The first is zero since $\sum_j p_j A_j = 0$ for a transverse vector potential, and the second contributes only to the longitudinal component. The surviving terms are of the third form and give

$$\Pi_{ij}^{(1)}(\vec{p}, p_0) = \int \frac{d^3q}{(2\pi)^3} (4E_q E_{q+p})^{-1} \{[nv_q nv_{q+p} - (T_q + E_q + nv_q)(T_{q+p} - E_{q+p} + nv_{q+p})]K^+$$

$$- [nv_q nv_{q+p} - (T_q - E_q + nv_q)(T_{q+p} + E_{q+p} + nv_{q+p})]K^-\} q_i q_j \ . \tag{45}$$

Because of the cylindrical symmetry, (45) is nonzero only when $i = j$, and thus (42) reduces to the London equation. In the static limit, we find

$$\Pi_{ij}^{(1)}(\vec{p}, 0) = -\tfrac{1}{2}\delta_{ij} \int \frac{d^3q}{(2\pi)^3} q_i^2 (E_q + E_{q+p})^{-1} \left[\frac{1}{2}\left(\frac{\lambda_q}{\lambda_{q+p}} + \frac{\lambda_{q+p}}{\lambda_q}\right) - 1\right] \ . \tag{46}$$

Clearly (46) is zero, in the limit $\vec{p} \rightarrow 0$ and $\vec{p} \rightarrow \infty$, and the paramagnetic term of the induced current is consequently zero. We refer the readers to Fetter's article for further discussions.

The diagrams in Fig. 3 have not been calculated yet. We plan to undertake this problem in the future. Whether or not the above-explained perfect Meissner effect persists even at the second order of approximation will be reported along with the result of $\pi^{(2)}$ in the future.

C. Ma-Woo formalism

The longitudinal component of the current correlation function may also be obtained from the diagrams in Figs. 1 and 2. For the reasons mentioned earlier, $\varphi_{33} = \Pi_{33}$, where the subscript 3 refers to the direction of $\vec{p}$. The function Π_{33} has been calculated by Ma and Woo (they call it F^{33}). The same result may be obtained by our method with a smaller degree of difficulty. One may proceed as for π keeping in mind again that the two external vertices represent $\vec{J}$ (this time it is the number current, not electric current, following Ma and Woo). It is sufficient just to write down the final result,

$$\Pi_{33}^{(0)}(p) = \frac{2nT_{\vec{p}}}{(p_0 - E_p + i\delta)(p_0 + E_p - i\delta)}\ \frac{p^2}{4m^2} \ , \tag{47}$$

$$\Pi_{33}^{(1)}(p) = [G_0^+(p) - G_0^+(-p)](\Gamma_+ + \Gamma_-)(p/2m^2) + [G_0^+(p) + G_0^+(-p)][(\Gamma_+ - \Gamma_-)(p/2m^2) + n_0^{(1)}(p^2/4m^2)]$$
$$+ (1/m^2)F^{33r} + G_0^+(p)G_0^+(-p)(-p^2/2m^2)M_2^{(1)} + [G_0^{+2}(p) + G_0^{+2}(-p)](S^{(1)} - \mu^{(1)})(p^2/4m^2)$$
$$+ [G_0^{+2}(p) - G_0^{+2}(-p)]A^{(1)}(p^2/4m^2) , \tag{48}$$

where

$$\Gamma_+ + \Gamma_- = \frac{1}{2}\int \frac{d^3q}{(2\pi)^3}\, nv_q(\lambda_q - \lambda_{q+p})(\hat{p}\cdot\vec{q} + \tfrac{1}{2}p)\, Q^- ,$$

$$\Gamma_+ - \Gamma_- = \frac{1}{2}\int \frac{d^3q}{(2\pi)^3}\, nv_q(\lambda_q/\lambda_{q+p} - 1)(\hat{p}\cdot\vec{q} + \tfrac{1}{2}p)\, Q^+ ,$$

$$F^{33r} = \frac{1}{4}\int \frac{d^3q}{(2\pi)^3}\, \lambda_q^{-1}(1 - \lambda_q)(\lambda_{p+q} - \lambda_q)(\hat{p}\cdot\vec{q} + \tfrac{1}{2}p)^2\, Q^+ ,$$

$$\tag{49}$$

$$M_2^{(1)} = \frac{1}{4}\int \frac{d^3q}{(2\pi)^3}\, nv_q[nv_{q+p}(\lambda_q\lambda_{q+p} - 1) + nv_q\lambda_q(\lambda_{q+p} - 1/\lambda_{q+p})]\, Q^+ + \frac{1}{4}\int \frac{d^3q}{(2\pi)^3}\, nv_{q+p}(\lambda_q - 1/\lambda_q) ,$$

$$S^{(1)} = \frac{1}{4}\int \frac{d^3q}{(2\pi)^3}\, nv_{q+p}(\lambda_q - 1)^2/\lambda_q + \frac{1}{4}\int \frac{d^3q}{(2\pi)^3}\, nv_q[nv_q(\lambda_q\lambda_{q+p} + \lambda_q/\lambda_{q+p}) + nv_{q+p}(\lambda_q\lambda_{q+p} + 1)]\, Q^+ ,$$

$$A^{(1)} = \frac{1}{2}\int \frac{d^3q}{(2\pi)^3}\, nv_q\lambda_q(nv_q + nv_{q+p})\, Q^- ,$$

with

$$Q^{\pm} = K^- \mp K^+ .$$

The functions defined in (49) are the same as defined by Ma and Woo. The continuity equation relates[3] Π_{33} to π by

$$\pi(p) = (p^2/p_0^2)(\Pi_{33} + n/m) . \tag{50}$$

Substituting $\Pi_{33}^{(0)}$ in (50) yields $\pi^{(0)}$. We have failed, however, to prove analytically whether or not the substitution of $\Pi_{33}^{(0)} + \Pi_{33}^{(1)}$ in (50) yields $\pi^{(0)} + \pi^{(1)}$. But the fact that the two numerical results of ΔE_p obtained from (50) and (20) agree with each other appears to indicate the equivalence of the two.

VI. CONCLUDING REMARKS AND SUMMARY

In this paper, we have derived the generalized dielectric constant of a dense charged boson gas to the order next to the Bogoliubov approximation. The method is based upon the fermion analogy which was first exploited by Brandow using the time-independent formalisms popular in the nuear matter and known by the names of Brueckner, Goldstone, and Bethe. The dielectric formalism in this paper uses the time-dependent formalism of Feynman and Dyson. Of course the time variable q_0 is eliminated at the end of each partial summation of diagrams. We have demonstrated sufficiently that retaining the time variable to the last stage instead of eliminating at the beginning is not by any means a disadvantage in dealing with a dense charged boson gas. In fact, if one compares, for example, the time-independent summation procedure for diagrams of N_0 shown in Ref. 6 with the time-dependent way shown in this paper, the latter

proves to be substantially simpler than the former. What is accomplished in the time-independent method by a delicate use of the factorization theorem is done in the time-dependent method by a trivial integration over the time variable.

In comparison with the dielectric formalism of Ma and Woo (MW) and the Green's-function approach of Schick and Wu (SW), we believe that the apparent simplicity of our procedure is more than a pedagogical interest. We wish to stress that those subsidiary correlation functions that the MW formalism requires to introduce and the tangle of μ and n_0, which is more apparent in the SW formalism, may all be handled "automatically" by the introduction of the "free particle-hole Green's function" G_0^-. In particular, the fact that right factors of μ and n_0 are calculated and put at right places automatically should prove to be a substantial advantage at the second order of approximation where $\pi^{(2)}$ would be included.

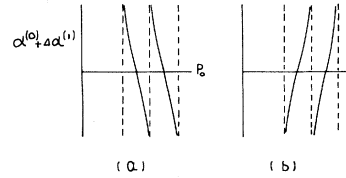The results of this paper may be summarized as

(a)   (b)

FIG. 8. Sketches for the possible intersections of the ordinate value unity with $\alpha_{\vec{p}}^{(0)}(p_0) + \Delta\alpha_{\vec{p}}^{(1)}(p_0)$ in the two-plasmon continuum region. The dotted lines represent $p_0 = E_{\vec{q}} + E_{\vec{q}+\vec{p}} = E_{-\vec{q}} + E_{\vec{q}+\vec{p}}$. (a) is the case for a dense charged boson gas.

follows:

(i) The first-order correction to the Bogoliubov excitation spectrum was obtained. This problem has received a considerable amount of interest recently by several authors.[15] We have shown that our result agrees with that of Ma and Woo numerically.

(ii) Damping of the plasmon state was examined. While this was done for an electron gas quite some time ago by DuBois, curiously enough no work has been done for a charged boson gas. We have computed the leading term.

(iii) We have proven that, up to the first order of approximation, there is only one mode of elementary excitation, and the second mode that Carmi and Lock claim to exist is absent.

(iv) We have proven that the nature of the screening of the system to a static impurity charge at $T = 0$ is, up to the first order of approximation, *exponential*. We have also presented a diagrammatic argument to show the perfect Meissner effect at the long- and short-wavelength limits.

(v) In an appendix, we have shown that the r_s expansion of n_0 contains only terms of integer powers of $r_s^{3/4}$; the $r_s^{9/8}$ term of Schick and Wu is absent.

From the generalized dielectric constant, it is possible to calculate the static structure function $S(p)$. There was a demand for a calculation of $S(p)$ to the order next to the Bogoliubov approximation. A dielectric calculation has been performed recently by Family[16] for this term of $S(p)$. Family performed another calculation using a collective coordinate method, and the result is in a striking agreement with that of the dielectric approach. Berdahl[17] has also carried out a calculation recently. His calculation is based upon the observation that $S(p)$ is related to the functional derivative of the ground-state energy with respect to the Fourier transform of the interaction potential. The result of Berdahl and the two results of Family are in agreement. Therefore this subject matter of $S(p)$ appears to be well settled.

One can also calculate in principle the ground-state energy from the dielectric constant. The leading term may be obtained by carrying out a trivial integration over the coupling constant.[4] The necessary integration over the coupling constant at the next order is, however, by no means simple; we do not find any advantage over the previous approaches.

Thus we will turn our effort to calculating the diagrams of $\pi^{(2)}$. The result should be interesting because the inclusion of $\pi^{(2)}$ would take the three plasmon intermediate states into account without any approximation.

ACKNOWLEDGMENTS

APPENDIX A: CHEMICAL POTENTIAL

The purpose of this and the next appendixes is to identify the two factors $\mu^{(1)}$ and $n_0^{(1)}$ appearing in (10) as the first-order expansion terms of the chemical potential and the condensate density $n_0^{(1)} = N_0^{(1)}/\Omega$, respectively. Such identification is not essential as far as our dielectric formalism is conserned, but μ and N_0 are important variables on their own rights and thus we wish to show that they (μ and N_0) may be calculated using the time-dependent perturbation scheme. As was mentioned in the Introduction, μ or N_0 may be computed to any order of approximation without having to know the other; whereas in the conventional perturbation method one cannot be calculated without the other, and more importantly the result of any calculation of μ (or N_0) will involve yet unknown μ (or N_0).

First consider the chemical potential μ. We start from $\mu = (\partial E_0 / \partial N)_\Omega$. Here E_0 is the ground-state energy and is given by

$$E_0 = \int_0^1 \frac{d\lambda}{\lambda} \langle \Psi_0(\lambda) | H_{1\lambda} | \Psi_0(\lambda) \rangle$$

$$= \int_0^1 \frac{d\lambda}{\lambda} \langle 0 | T(H_{1\lambda} S(\lambda)) | 0 \rangle_L \,, \qquad (A1)$$

where $H_{1\lambda}$ is the potential-energy operator with coupling given by $\lambda v_{\vec{q}}$; $S(\lambda)$ is the time-evolution operator $\hat{U}_\lambda(\infty, -\infty)$; $| \Psi_0(\lambda) \rangle$ and $| 0 \rangle$ are the interacting and noninteracting ground state, respectively; L indicates that only linked diagrams be taken. To the zeroth order of approximation, E_0 is given by ring diagrams. With some care not to double count, one can find

$$E_0^{(0)} = i \frac{\Omega}{2} \sum_{l=2}^\infty \frac{1}{l} \int \frac{d^4q}{(2\pi)^4} [v_{\vec{q}} \pi^{(0)}(q)]^l \,, \qquad (A2)$$

where we have carried out the λ integration. Each π contains a Fermi loop and thus has a factor of $-N$. By differentiating (A2) with respect to N, the awkward factor $1/l$ is cancelled with the result

$$\mu^{(1)} = \tfrac{1}{2} i n^{-1} \sum_{l=2}^\infty \int \frac{d^4q}{(2\pi)^4} [v_{\vec{q}} \pi^{(0)}(q)]^l \,. \qquad (A3)$$

The series may be summed and then, by using the second line of (4), is reduced to (11).
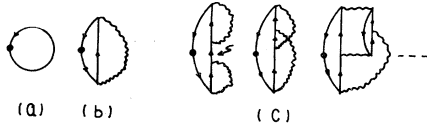
FIG. 9. Perturbation expansion for $N_0 = \langle a_0^\dagger a_0 \rangle$: (a) $N_0^{(0)}$, (b) $N_0^{(1)}$, (c) $N_0^{(2)}$. The wiggly lines represent $\nu_{eff}(p)$ given by (7). The curly arrow has been drawn for a purpose of reference in Appendix C.

The zeroth-order term $\mu^{(0)}$ is zero for a charged system since the corresponding E_0 is zero. For the succeeding higher-order terms, one can continue with the diagrams with total independent momentum variables equal to two, three, four, and so on. The counting problem becomes somewhat involved but the final result is the same as (A3), with $\pi^{(0)}$ replaced by π. We should note, however, that the $\pi^{(0)}$ in (A2) may not be replaced by π. The exact result is

$$\mu = \frac{i}{2} n^{-1} \int \frac{d^4 q}{(2\pi)^4} \pi(q) \nu_q^2 F(q) . \tag{A4}$$

The contribution of $\mu^{(l)}$ is clearly of order $r_s^{-3/2}$ $(r_s^{3/4})^l$.

APPENDIX B: NUMBER OF PARTICLES IN THE CONDENSATE

We consider here N_0, the number of particles in the condensate. We start from

$$N_0 = \langle a_0^\dagger a_0 \rangle = \langle 0 | T(a_0^\dagger(0) a_0(0) S) | 0 \rangle_L . \tag{B1}$$

One might call it a "hole Green's function" $iG^-(\vec{p} = 0, t = 0)$, and we wish to take this view. Perturbation terms of (B1) may be shown as in Fig. 9, where (a), (b), (c) correspond to $N_0^{(0)}$, $N_0^{(1)}$, and $N_0^{(2)}$, respectively. The two external lines which are represented by G_0^- are tied together by a dot because $a_0^\dagger$ and a_0 act at the same time. This is not merely for a style but is essential to apply the fermion analogy correctly. We find, up to the first order,

$$N_0^{(0)} = \langle 0 | a_0^\dagger a_0 | 0 \rangle = N ,$$

$$N_0^{(1)} = i^2(-N) \int \frac{dq_0}{(2\pi)} [G_0^-(q)]^2$$

$$\times \int \frac{d^4 k}{(2\pi)^4} G_0^+(\vec{k}, k_0 + q_0) \nu_{eff}'(k) \tag{B2}$$

$$= -iN \int \frac{d^4 k}{(2\pi)^4} [G_0^+(k)]^2 \nu_{eff}'(k)$$

$$= -N \int n^{-1} \frac{d^3 k}{(2\pi)^3} f_{\vec{k}} ,$$

where $f_{\vec{q}}$ is given by (19). The desired identification has been made. The function $f_{\vec{q}}$ represents the fraction of particles in the plane wave state $\vec{q}$.

This may be seen by examining $N_{\vec{q}} = \langle a_{\vec{q}}^\dagger a_{\vec{q}} \rangle$ in the same way as for N_0. It is easy to find $N_{\vec{q}}^{(0)} = 0$, $N_{\vec{q}}^{(1)} = N f_{\vec{q}}^{(1)}$. Clearly $N_0^{(1)}$ is of order $r_s^{3/4}$.

The diagrams of $N_0^{(2)}$ are shown in Fig. 9(c). In these diagrams, there are two independent momentum variables and therefore they contribute to the order of $r_s^{(3/4)\times 2}$. In general, diagrams of $N_0^{(l)}$ have l-independent momentum variables and therefore contribute to the order of $(r_s^{3/4})^l$.

We have mentioned this because according to Schick and Wu,[13] N_0 has a term of order $r_s^{9/8}$. The presence of such terms in N_0 would imply that the ground-state energy and μ also contain similar terms of noninteger power of $r_s^{3/4}$. In Ref. 6, we have shown that the ground-state energy contains only terms of integer power of $r_s^{3/4}$. In Appendix A, we have also shown that the chemical potential contains only terms of integer power of $r_s^{3/4}$. Therefore, it is our belief that the $r_s^{9/8}$ term is absent in the expansion of N_0.

APPENDIX C: CONNECTION TO THE FORMALISM OF HUGENHOLTZ AND PINES

This subject matter has been explained by Brandow in a time-independent way. Since he has put the main emphasis on the problems of the ground-state energy, we will provide here an equivalent argument for the correlation function F in a time-dependent way.

In the formalisms of Hugenholtz and Pines (HP), there is no hole line, but instead one multiplies the factor $N_0^{1/2}$ for every replaced (by $N_0^{1/2}$) condensate operator, and a directed line represents

$$G_0(p) = (p_0 - T_{\vec{p}} + \mu + i\delta)^{-1} . \tag{C1}$$

It differs from our G_0^+ by the factor μ in the denominator. At the order of Bogoliubov approximation, F is given by[2]

$$F_a(p) = n_0 [G_{11}(p) + G_{11}(-p) + G_{12}(p) + G_{12}(-p)]. \tag{C2}$$

Diagramatically it is represented by Fig. 10. It is easy to see that with N_0 set to N, F_a is equal to our $F^{(0)}$. Recalling that $\pi^{(0)}(p) = nG_0^+(p) + nG_0^+(-p)$, it is also easy to see what each term in (C2) refers to: if the first and the last $\pi^{(0)}$ diagrams in our $F^{(0)}$ are $nG_0^+(p)$, the result reduces to G_{11}; if both are $nG_0^+(-p)$, we have $G_{11}(-p)$; if one of the two (ei-
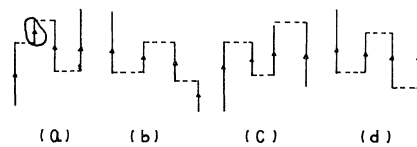

FIG. 10. Typical diagrams of (a) $G_{11}(p)$, (b) $G_{11}(-p)$, (c) $G_{12}(p)$, (d) $G_{21}(p)$. The dotted lines are $\nu_{\vec{p}}$, not $\nu_{eff}(p)$. The circle in (a) is for a purpose of reference in Appendix C.

ther first or last) is $nG_0^+(p)$ and the other is $nG_0^+(-p)$, it reduces to the last two anomalous terms.

Now we pick up just one segment of a diagram such as enclosed by a circle in Fig. 10(a). The contribution of this portion of the diagram is given by (C1) multiplied by n_0. How does the factor N change to N_0 and how does the factor μ sneak into the denominator? This may be done by adding diagrams of higher orders to $\pi^{(0)}$. Among the diagrams of $\pi^{(1)}$, choose Fig. 2(b). In this diagram, a directed line may be either G_0^+ or G_0^-. Now take a partial contribution (PC) of this diagram by letting the two indicated lines (by curly arrows) be G_0^-. This PC has already been calculated in the last two terms of (10). Next go to $\pi^{(2)}$. Choose the diagram with two "bumps" in Fig. 3 and calculate the PC by letting the three indicated lines be G_0^-. Continue with the diagram of $\pi^{(3)}$ with three bumps, and so on. The PC of each is

no-bump diagram $= G_0^+(p)n_0^{(0)}$,

one-bump diagram $= [G_0^+(p)]^2(-\mu^{(1)})n_0^{(0)} + G_0^+(p)n_0^{(1)}$,

$$ \hspace{10em} \text{(C3)} $$

two-bump diagram $= [G_0^+(p)]^3(-\mu^{(1)})^2 n_0^{(0)}$

$$ + [G_0^+(p)]^2(-\mu^{(1)})n_0^{(1)} $$

$$ + G_0^+(p)n_0'^{(2)}, \cdots, $$

where $n_0'^{(2)}$ represents the partial contribution that the first diagram in Fig. 9(c) makes to $n_0^{(2)}$ when the indicated line is G_0^-. The sum of (C3) is given by

$$ G_0^+(p)(n_0^{(0)} + n_0^{(1)} + \cdots) $$

$$ + [G_0^+(p)]^2(-\mu^{(1)})(n_0^{(0)} + n_0^{(1)} + \cdots) $$

$$ + [G_0^+(p)]^3(-\mu^{(1)})^2(n_0^{(0)} + n_0^{(1)} + \cdots) + \cdots . \quad (4) $$

The series is summed easily to the desired result.

Two very awkward and rather dangerous affairs have been done: (i) only one diagram has been chosen at each order when the rest make contributions of equal order. (ii) Even the chosen diagram was not allowed to make its *full* contribution. These are justified only for the Hamiltonian of Bogoliubov, which contains two condensate operators in the interaction term. For the Hamiltonian of Bogoliubov, the diagrams not included and mentioned in (i) are all zero, and the rest of the contributions of the chosen diagrams mentioned in (ii) are also zero. As one includes the terms of Hamiltonian that Bogoliubov dropped, there emerge, in addition to F_a, F_b and F_c (in the notation of Hugenholtz and Pines). The above analysis may be extended to higher orders but the details are not illuminating; the notations adopted in (17) and (18) and the algebra from there on is sufficient.

[1]D. Pines, *The Many-Body Problems* (Benjamin, New York, 1961).

[2]N. M. Hugenholtz and D. Pines, Phys. Rev. 116, 489 (1959).

[3]S. K. Ma and C. W. Woo, Phys. Rev. 159, 165 (1967).

[4]J. C. Lee, Phys. Rev. B 5, 1925 (1972).

[5]B. H. Brandow, Phys. Rev. Lett. 22, 173 (1969); Ann. Phys. (N.Y.) 64, 21 (1971).

[6]J. C. Lee, Phys. Rev. B 4, 2050 (1971).

[7]M. Gell-Mann and K. A. Brueckner, Phys. Rev. 106, 364 (1957).

[8]D. F. DuBois, Ann. Phys. (N.Y.) 7, 174 (1959); 8, 24 (1959). There are many other works of dielectric approach to electron gas, but we have made no effort to provide a complete list.

[9]A. L. Fetter and J. D. Walecka, *Quantum Theory of Many-Particle Systems* (McGraw-Hill, New York, 1971),

p. 102. The only difference is that $k_F = 0$ and the total spin degeneracy is N instead of 2. We will set $\hbar = 1$.

[10]G. Carmi and A. J. Lock, Phys. Rev. B 5, 1447 (1972). They call it single-particle excitation spectrum.

[11]The screening effect was discussed both at and above the phase transition temperature by A. L. Fetter [Ann. Phys. (N.Y.) 64, 1 (1971)].

[12]A. L. Fetter, Ann. Phys. (N.Y.) 60, 464 (1970).

[13]M. Schick and T. M. Wu, Phys. Rev. 177, 313 (1969).

[14]C. W. Woo and S. K. Ma, Phys. Rev. 159, 176 (1967).

[15]Refs. 3 and 14; D. K. Lee, Phys. Rev. B 8, 2735 (1973); J. P. Straley, *ibid.* 6, 498 (1972); A. Bhattacharyya and C. W. Woo, Phys. Rev. Lett. 28, 1320 (1972); Phys. Rev. B 7, 204 (1973).

[16]F. Family, Ph.D. thesis (Clark University, 1974) (unpublished).

[17]P. Berdahl (private communication).